International Journal of GEOMATE, June 2019, Vol.16, Issue 58, pp.203 - 210
Geotec., Const. Mat. & Env., DOI: https://doi.org/10.21660/2019.58.82002
ISSN: 2186-2982 (Print), 2186-2990 (Online), Japan

BEHAVIORS OF CRACK PROPAGATION OF ROCK-LIKE MATERIAL WITH DIFFERENT JOINTED THICKNESS

Pham Thi Nhan[1]*, Xu Xi[2], Sanda Suresh[3]

[1]Department of Civil engineering, Hanoi University of Mining and Geology, Vietnam; [2]Taizhou maritime safety administration People's Republic of China; [3]Kabeli Energy Limited, Buddhanagar, Kathmandu, Nepal

*Corresponding Author, Received: 24 Oct. 2018, Revised: 29 Dec. 2018, Accepted: 13 Jan. 2019

ABSTRACT: To better understand the interaction of joints and its effect on the mechanical behavior of jointed Rock-like material models, the results of a physical experiment program undertaken in the laboratory were present in this manuscript. This experiment used the physical simulation method to study the mechanical and acoustic properties of specimens. The ratio of cement: sand (quartz stone): water = 1:2:0.5 respectively was used to make 100 ×100×100 mm of jointed cubic specimens. Based on the uniaxial load test of a single jointed rock mass model, the relationship between the jointed thickness and the peak strength is obtained. The result shows that the peak strength decreased with the increase of joint thickness. At the same time, by using acoustic emission on fracture procession and digital photographic analysis, obtained acoustic emission events localization and fracture propagation characteristics in jointed rock mass with the different joint. It is found that in different stages of the stress-strain curve, the acoustic emission signals show the varying degrees of intensity. At the beginning of plastic deformation and strain softening propagation, the ring-down counting will be suddenly increased and the cluster location depends on the joint. The failure modes of the specimens with different jointed thickness were mainly the splitting failure and partial shear failure.

Keyword: Joint thickness, Acoustic Emission, Failure mode, Ring-down count

1. INTRODUCTION

Study on the strength failure and crack coalescence behavior of rock material containing different pre-existing cracks (fissures, holes, combined flaws) has been a significant topic in current research. There are numerous experimental investigations on crack initiation and coalescence of pre-cracked rock. Most of the work [1-4] have been focused on a physical test of real rock specimens such as brittle rock. YANG et al [1] investigated the brittle sandstone specimens containing a single fissure and obtained that the strength and deformation failure behavior of rock were depending on single fissure length and fissure angle.

YANG et al [2] by using Uniaxial compression test and Acoustic Emission (AE) techniques for red sandstone specimens which contain two unparallel fissures in order to study the effect of fissure angle on the mechanical behavior and also analyzed the real-time crack coalescence process.

In nature, engineering rock masses do not always contain parallel fissures and generally composed of unparallel fissures. Many previous studies have focused on crack coalescence between non-parallel flaws as well [3-5]. Lee and Jeon [4] carried out uniaxial compression experiment for Diastone (types of molded gypsum) and granite containing two unparallel fissures. This study was a good start to consider the coalescence of non-parallel flaws, but it is not sufficient to only study configurations in which one flaw is partially or completely underneath the other horizontal flaw. Zhang et al. [5] also studied the coalescence behavior of non-parallel flaws and their results identified five types of linkage between the two flaws: tensile crack linkage with shear coalescence at the tip, shear crack linkage, mixed linkage, tensile crack linkage, and indirect crack linkage.

Besides the above typical tests on model materials containing cracks, some specimens contained combined flaws, have also been tested to investigate the mechanical behaviors of precracked rock materials. Li et al [6] carried out the uniaxial compression experiments on marble with combined flaws, to investigate the propagation and coalescence of cracks in marble specimens. The result showed that two types of newborn cracks are observed: wing (tensile) cracks and secondary (shear) cracks. Sheng-qi Yang [7] based on the axial stress-axial strain curves, the effect of fissure angle on the strength and deformation behavior of sandstone specimens containing combined flaws is analyzed. According to the monitored results, the effect of crack coalescence process on the strength and deformation behavior is investigated based on a detailed analysis of brittle sandstone specimens containing combined flaws by using digital photogrammetry. Qian Yin [8] focused on the effect of pre-existing flaw geometry on mechanical behavior and crack coalescence modes of the sandstone specimens containing combined flaws with different fissure angle, ligament length and fissure length under uniaxial compression. The effect of flaw geometry on the mechanical behavior of sandstone specimens was analyzed.

In order to investigate the influence of water chemistry on the mechanical behavior of pre-fissure red sandstone, Lu. et . al [9] based on the results of the uniaxial compressive test on cylindrical red sandstone under chemical action was done, which provided a clear understanding of the effect of strength and deformation characteristics, and major modes of crack coalescence in cracked rocks. By the numerous experimental study, Feng et. al [10] investigated the mechanism of multi-crack interaction in limestone specimen, where the size of the specimen was 15mm×30mm×3mm, contained with two or three fissures of different arrangements under the coupled uniaxial compressive stress and chemical solutions with different ionic concentrations and pH values. The results of the experiment showed that apart from mineral components of rock and the number of flaws, the influence of complicated chemical corrosion depending on pH values, chemical ions, and their concentrations.

The interaction between multiple pre-existing flaws and its effect on the mechanical behavior of rock or rock-like specimens were considered in previous studies, such as the joint inclination angle, joint distance [11-16], and overlap distance [13-14].

Many numerical methods have been developed and applied to simulate the mechanical behavior of non-persistent jointed rock mass and had been extensively investigated through numerical modeling[16-18]. Fan et al [16] by using PFC3D software [17], performed numerical simulations to study the influence of multi-non-persistent joints on jointed rock block mechanical behavior. The result showed the significant influence of joint orientation and its persistence on the strength and deformation modulus values of jointed rock blocks. Yang et. al [18] by numerical simulations investigated the mechanical behavior of a jointed rock mass with non-persistent joint orientation and support stress on the free surface on mechanical behavior and three failure modes identified are intact rock failure, step-path failure, and planar failure.

As it is well known, acoustic emission (AE) technique is an efficient measuring tool to present the evolution and propagation of defects in materials and has been widely applied to investigate the internal damage and fracture behavior of the rock material in many types of studies [19-21]. However, AE techniques were less used to date to explore the initiation, propagation, and coalescence of rock-like specimens containing flaws.

In this manuscript, the results of a laboratory experimental program designed to look at the interaction of joints and its effect on the failure mode, strength and deformation behavior of jointed rock masses are presented. The acoustic emission characteristics and fracture evolution of jointed rock mass with different jointed parameters are studied under uniaxial compression.

2. MECHANICAL PROPERTIES OF SPECIMEN

After the multiple numbers of experimental test, the material composition ratio was determined as follows: Cement to sand (Quartz) mass ratio is 1:2, water is 1/5 of the total weight. The experimental results are shown in the following table:

Table 1 Test results of experimental parameters under uniaxial compression

Mass ratio	Specimen number	Diameter d (mm)	Height h (mm)	Weight m (g)	Bulk density γ (KN/m^3)	Compressive strength σ_c (MPa)	Elastic Modulus E(GPa)
S 1:2	1-2-1	50.01	99.00	398.46	20.49	25.72	2.92
	1-2-2	50.15	98.40	404.26	20.80	30.84	3.08
	1-2-3	50.14	98.71	399.81	20.51	26.00	3.45
	1-2-4	50.18	97.21	397.00	20.65	24.05	2.75

Table 2 Table Test results of tensile strength parameters

Specimen number	Tensile strength (σ_t/MPa)	
	Test value	mean value
S1-2-5	3.73	
S1-2-6	3.62	3.72
S1-2-7	2.99	

The test ratio which gave the experiment result with minimum stability error was selected. Experimental damage formed were mainly tensile, and shown as below:

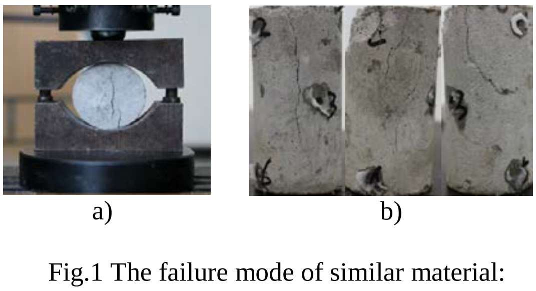

a) b)

Fig.1 The failure mode of similar material: a) Shear test; b) Uniaxial compression

The method for making jointed rock specimen: During the process of pouring the C:S mixture in the specimen mould, a constant dip angle and depth of stainless steel sheet with different thickness into the model was carefully maintained, and the metal sheet was extracted before solidification of C:S mixture model. It was quite challenging to accurately control the surface position and the corresponding depth of the joint. The author succeeds through the continuous attempt to groping the poured specimen. A test method for the production of jointed rock specimens was designed independently. The method is simple to operate, completed the model of specimen effect is better. The materials required for this method were included: 100 mm×100 mm×100 mm plastic mold, silicone gasket, washers, stainless steel, and stainless steel plate. Production experiment tools and the process is shown in (Fig.2).

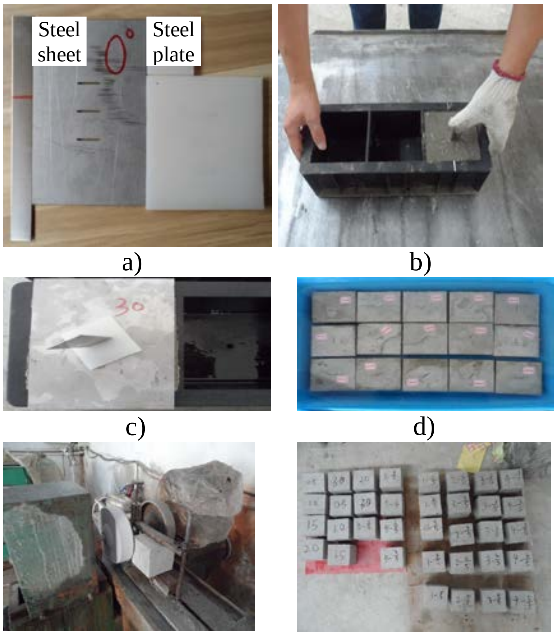

a) b) c) d) e) f)

Fig.2 The production tools and processes of Specimens: a) Tools; b) Vibration; c) Prefabricated joints; d) Maintenance; e) Polish; f) forming

All experiments were done at the State Key Laboratory for Geomechanics and Deep Underground Engineering, China University of Mining and Technology. The test loading system using YNS-2000 type electro-hydraulic servo testing machine was obtained as shown in (Fig.3). Axial displacement was controlled to keep the rock-like specimens in a quasi-static state under compression rate of 0.0025 mm/s. The axial force and displacements were recorded automatically by the loading equipment. The petroleum Vaseline gel was applied on both sides upper and lower loading face of mainframe pressing machine to minimize the frictional loss.

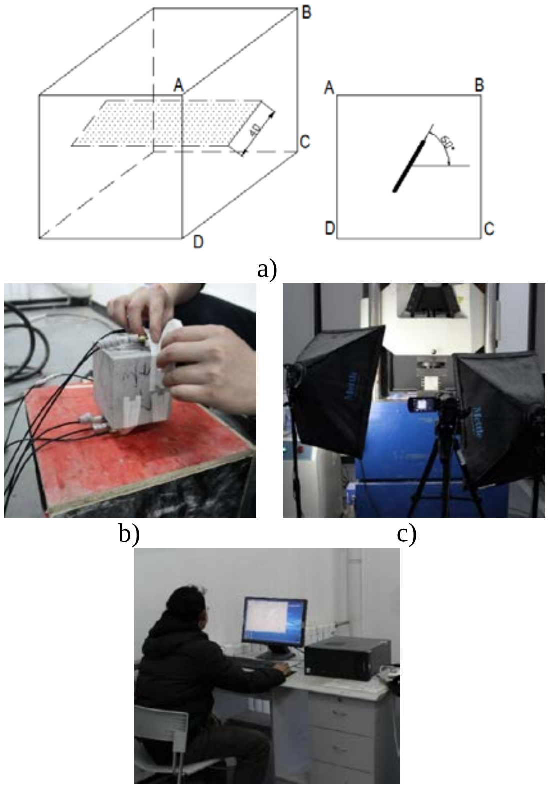

a) b) c) d)

Fig.3 Electro-hydraulic servo testing system of YNS-2000.
a) A simplified model of the jointed specimen; b) Fixed probe; c) Loading system; d) control system

3. TEST RESULTS

3.1 Stress-strain Curves of Specimens with A Different Joint Thickness

The joint of 40 mm width and 60-degree angle to horizontal was created throughout the length of the sample and it is shown in the Fig.3a. When the joint thickness is respectively 0.5 mm, 1.0 mm, 1.5 mm, 2.0 mm and 3.0 mm, the stress-strain curve of a single jointed rock mass under uniaxial compression is shown in Fig.4. From the figure, it can be seen that the stress-strain curves of single joint rock mass with different joint thickness include five stages: Compaction stage, elastic deformation stage, plastic deformation stage, strain softening stage and residual strength stage. The transitional stage in the curve of elastic deformation stage and the plastic deformation stage, the curve decrease gradually. This is mainly because at this time both sides of the specimen began to fracture and formed a larger macro fracture surface. In addition, when the jointed thickness increases, the peak stress reduction on the curve will become more and more distinct.

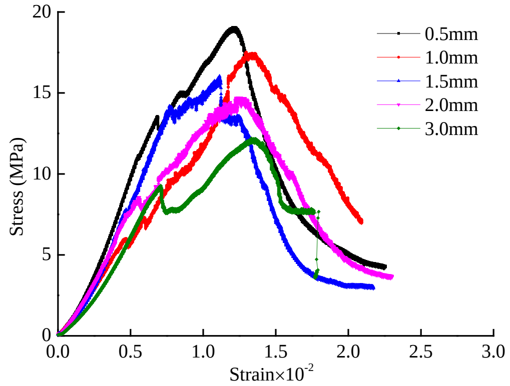

Fig.4 Stress-strain curves of the specimen with a different jointed thickness

3.2 The Relation Curve between E, ε_c, σ_c, and Joint Thickness

The values from the stress-strain curve (Fig. 5), for the elastic modulus (E), the peak strain (ε_c) and the peak stress (σ_c) of the single jointed rock mass in different jointed thickness are shown in table 3.

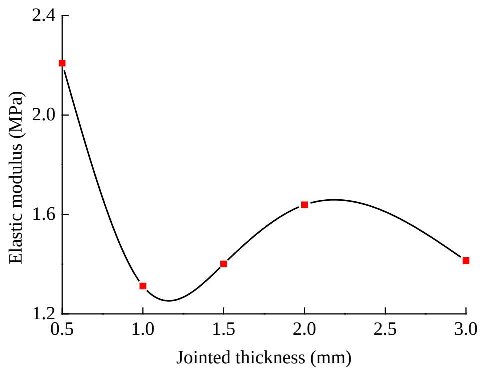

Fig.5 (a) *E*- Jointed thickness curve

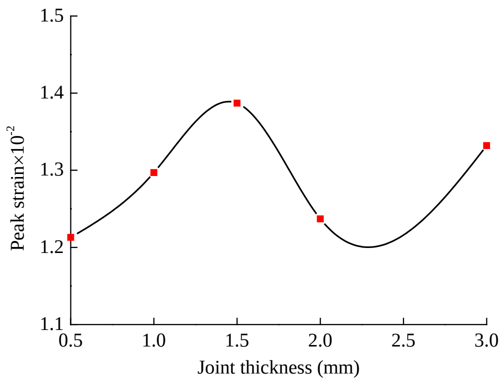

Fig.5 (b) ε_c- Jointed thickness curve

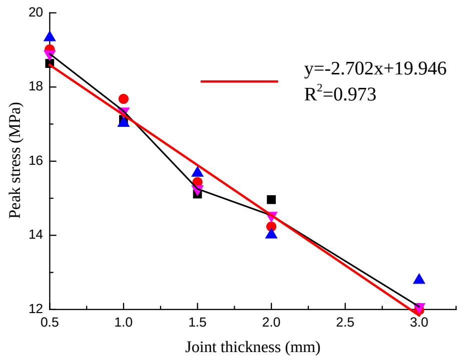

Fig.5 (c) σ_c- Jointed thickness curve

Fig.5 The relationship between E, ε_c, σ_c and jointed thickness curve

Table 3 The mechanical parameters table of the specimen with different joints thickness

Joint thickness /mm	0.5	1.0	1.5	2.0	3.0
E/GPa	2.209	1.312	1.387	1.639	1.414
$\varepsilon_c/10^{-2}$	1.213	1.297	1.401	1.237	1.332
σ_c/MPa	18.895	17.351	15.253	14.537	12.076

As per the (Fig.5) (a), the experiment result showed that with the increase in thickness of the joint, the elastic modulus of the single jointed rock mass quickly decrease at first, then increase gently up to a certain stage and finally decrease gently. When the thickness of the joint increased from 0.5 mm to 1.0 mm, large variations in elastic modulus takes place, that is a decrease from 2.209 GPa to 1.323 GPa, which is 40.1 % of initial value. Meanwhile, when the thickness of the joint increased from 1.0 mm to 2.0 mm, elastic modulus also gently increased from 1.323 GPa to 1.639 GPa, that is increased by 23.89% of the later larger value.

Here, the Figs. 5 (a), (b) and (c) show the correlation of the elastic modulus, the maximum strain, and the maximum stress with the varied thickness of the joint. In general, when the thickness of joint in specimens increased, the peak stress (σ_c) value seems to be linearly decreased approximately, whereas the elastic modulus and the peak strain values show non-linear behavior due to the effects of different joint thicknesses. But it is seen that the peak value of stress and the modulus of elasticity of specimen containing joints are significantly lower than no joint specimen.

3.3 Analysis of the Characteristics of the Expansion and Evolution of the Joint

To study the influence of the joint thickness in the fracture evolution of rock mass during the uniaxial compression process, the data of three typical features point image were analyzed on the test process.

The three points a) the crack initiation strength (σ_P), b) peak strength (σ_c) and c) post Peak strength ($0.5\sigma_c$) were studied successively. The fracture evolution characteristics of rock specimens under different joints thickness can be observed from Fig. 6-10 as shown.

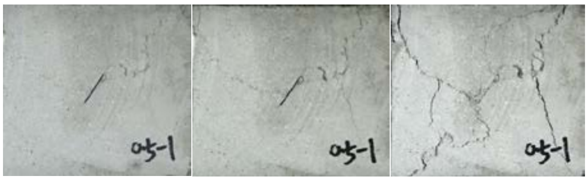

a) b) c)

Fig.6 The rupture evolution in 0.5 mm jointed thickness: a) Starting fracture $\sigma_p = 74.77\%\sigma_c$; b) Peak value σ_c; c) The post-peak $50\%0\sigma_c$

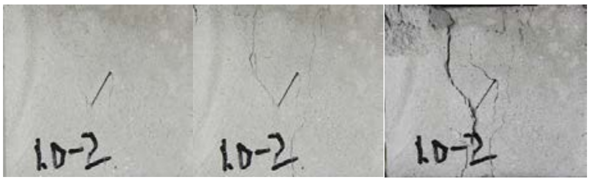

a) b) c)

Fig.7 The rupture evolution in 1.0mm jointed thickness: a) Starting fracture $\sigma_p = 85.86\%\ \sigma_c$; b) Peak value σ_c; c) The post-peak $0.5\%\sigma_c$

a) b) c)

Fig.8 The rupture evolution in 1.5 mm jointed thickness: a) Starting fracture $\sigma_p = 78.99\%\ \sigma_c$; b) Peak value σ_c; c) The post-peak $0.5\sigma_c$

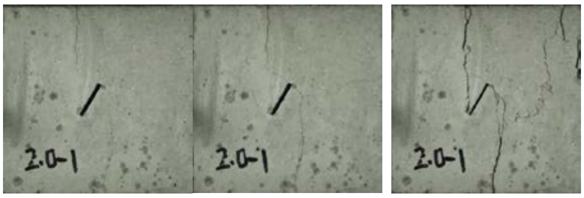

a) b) c)

Fig.9 The rupture evolution in 2 mm jointed thickness: a) Starting fracture $\sigma_p = 74.77\%\ \sigma_c$; b) Peak value σ_c; c) The post-peak $0.5\sigma_c$

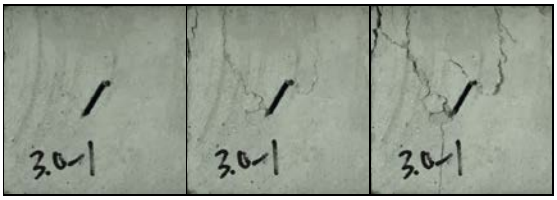

a) b) c)

Fig.10 The rupture evolution of 3 mm jointed thickness: a) starting fracture $\sigma_p = 71.05\%\ \sigma_c$; b) Peak value σ_c; c) The post-peak $50\sigma_c$

Again, the fracture evolution process of specimens under the different joints thickness conditions showing the order of cracks appearance sequentially can be observed from the (Fig.11), with the sequence of ascending order.

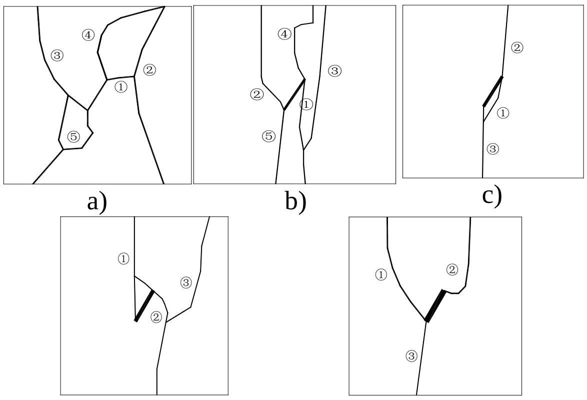

Fig.11 The sketch of failure modes in specimens with different joints thickness: a) 0.5 mm; b) 1 mm; c) 1.5 mm; d) 2 mm; e) 3 mm.

Under uniaxial compression, in the beginning, the failure of the specimen is mainly concentrated on the two lateral sides of the specimen. When the stress reaches the initial stage of plastic deformation, it is found that the stress decreased simultaneously, and both sides of the specimen are observed with a vertical splitting crack. And on the continuous increase in the pressure, the splitting crack on both sides also continued to extend from the top to bottom surface of the specimen, hence, observe tensile fracture surface. Meanwhile, when the joint thickness was less than or equal to 1.5 mm, the fractured surface side of the specimen was less which was mainly in the boundary of the specimen. Similarly, when the thickness was greater than 1.5 mm, the side of the specimens had produced several fractures through the surface, and the location was located in the middle of the specimen.

The specimen under continuous compression produced several destructed small blocks, and the final failure mode is in "cone" shape. When the joint thickness was less than 1.0 mm, the failure of the front face of the specimen was mainly caused by the multiple shear-compression fracture surface, and the failure mode was mainly a shear-compression failure, and the specimen produced more broken small pieces. When the thickness of joints is between 1.0 and 1.5, the failure of specimens is mainly caused by vertical macro-fracture surface from top to bottom along the longitudinal direction of joints. The failure mode is mainly splitting failure, and the surface of specimens will produce local spalling phenomenon.

When the thickness of the joint was greater than 1.5 mm, the failure mode observed mainly was compression shear and tensile failure, and the larger portion of the specimen was found to be broken, hence, the complete degree of the specimens was poor. Hence, when the joint thickness is, even more, larger, the number of crack on the surface of a damaged specimen is even lesser.

Meanwhile, the relationship between joint thickness and peak strain, as observed from the (Fig.5b), show that with the increase in the thickness of joint, the changing of the peak strain of the single jointed rock mass is rise and fall manner, but on the whole, initially, it shows a trend of increasing, then decreasing and again increasing trend. During the increase from 0.5 mm to 1.5 mm, the peak strain increase from 1.213 to 1.401, that is 15.50 % of initial value. Similarly, when the thickness of the joint increased from 1.5 mm to 2.0 mm, the peak strain decreased from 1.401 to 1.237, that is -11.71% of initial value. And, when increase from 2.0 mm to 3.0 mm, the peak strain increase from 1.237 to 1.332, which is 7.68 % of initial value.

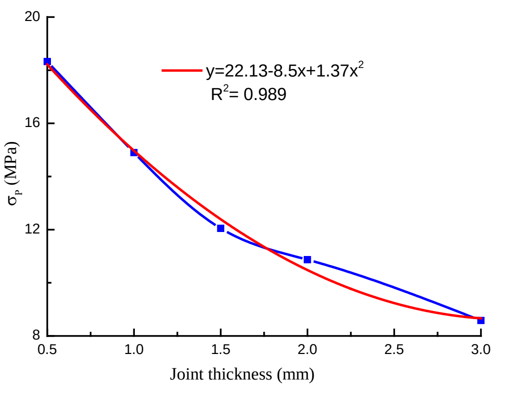

Fig.12 The curves between σ_p and jointed thickness

Similarly, the relationship between initial crack stress (σ_P) and joint thickness as observed from fig.12, it is observed that as the thickness of precast joint increases, the initial cracking stress fall gradually. When the jointed thickness increased from 0.5 mm to 3.0 mm, the initiation stress decreased from 18.324 MPa to 8.580 MPa, which is reduced by 53.18 %. On fitting the polynomial equation of initial crack stress and jointed thickness, the relationship between them satisfied the polynomial function, with the correlation coefficient R^2 = 0.989. As per this polynomial function, it can be speculated that when specimen containing 0 mm jointed thickness, the initial cracking stress of the specimen was 22.13 MPa. Thus, for similar materials types, this polynomial function is supposed to predict the crack stage.

3.4. Analysis of Acoustic Emission Signal Characteristics of Specimens under Uniaxial Compression Testing.

The typical relations between stress and ring-down count in varied time under different joints thickness are shown in (Fig.13).

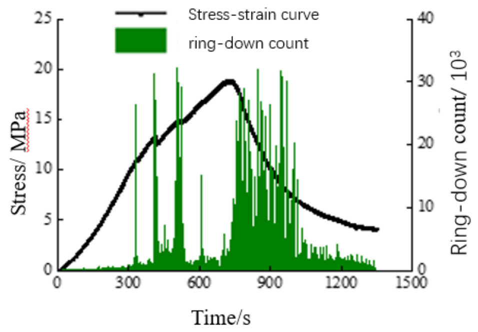

Fig.13a) Joint thickness = 0.5 mm

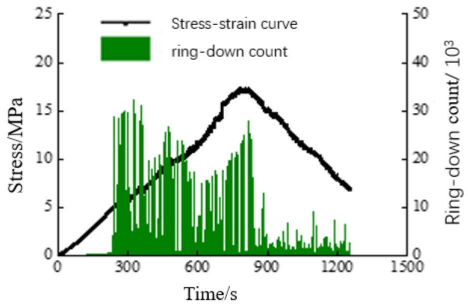

Fig.13b) Joint thickness = 1.0 mm

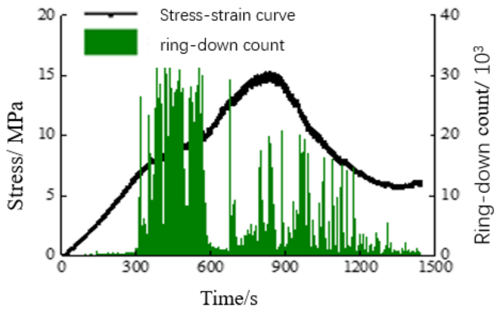

Fig.13c) Joint thickness = 1.5 mm

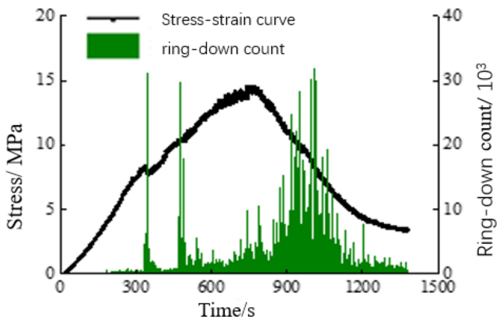

Fig.13d) Joint thickness = 2.0 mm

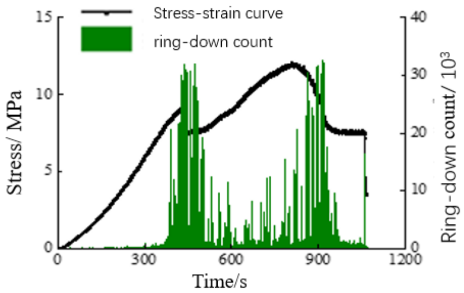

Fig.13e) Joint thickness = 3.0 mm

Fig.13 The typical relations of stress and ring-down count changing with time under different joints thickness.

The analysis of acoustic emission characteristics under the different thickness of the joint is also clearly shown in (Figs.13a-e).

At the beginning of loading, that is in the compaction stage, the acoustic emission (AE) signal is very weak up to the elastic stage. Very small ring-down counts are observed almost near to zero value. Suddenly, when curve reaches the elastic limit stage, the acoustic emission signals have significant enhancement and the ring-down count had a significant jump, this may be due to sudden failure (cracked development) with larger sound on the sample. Similarly, when the curve reaches the peak value (Ultimate Stress points), the ring-down count is much larger than other and several fluctuating jumps are observed. The ring-down count does not increase sharply close to the peak stress, and especially in the strain softening stages many AE events still emerge. This stage of specimen failure is relatively serious, and the surface of the specimen had been broken in more surface. Additionally, AE events reduce gradually with stress increase before reaching the peak. After the stress enters the strain softening stages, the acoustic emission signal becomes weak, the ringing count decreases and tends to be stable.

Thus, by the comparative study between the AE characteristics curve of pre-peak and post-peak stress is an advantageous way of identifying the peak stress.

4. CONCLUSIONS

Through uniaxial loading tests of single joint rock mass model, the relationship between different joint thickness and the peak stress intensity is obtained. When the thickness of the joint increases from 0.5 mm to 3.0 mm the peak strength, elastic modulus and peak strain will be decreased. Linear fitting of peak strength and joint thickness show that the relationship between them satisfies the linear function, but the elastic modulus and peak strain have varied extreme points.

The nature of the failure of the specimens with different joint thickness has the splitting failure in majority whereas shear failure in partly.

By the analysis on using both acoustic emission (AE) and digital photography during the rupture stages, the study of the location of acoustic emission and fracture characteristics under different parameters of joints are obtained. At the beginning of plastic deformation and strain softening propagation, the ring-down counting will sharply be increased and the cluster location depends on the joint thickness.

REFERENCES

[1] Yang S Q, Jing H W. Strength failure and crack coalescence behavior of brittle sandstone specimens containing a single fissure under uniaxial compression [J]. International Journal of Fracture, 2011, 68(2), pp227-250.

[2] Sheng-Qi Yang, Xiang-Ru Liu, Hong-Wen Jing. Experimental investigation on fracture coalescence behavior of red sandstone containing two unparallel fissures under uniaxial compression. International Journal of Rock mechanics and mining sciences, 2013, 63, pp82-92.

[3] Lajitai E. Z, Carter BJ, Duncan EJS. En echelon crack-arrays in Postash salt rock. Rock Mech Rock Eng 1994;27, pp89-111.

[4] Lee H, Jeon S.An experimental And numerical study of fracture coalescence in pre-cracked specimens under uniaxial compression. Int J Solids Struct 2011;48(6), pp979-99.

[5] Zhang X.P, Q.S. Liu, S.C. Wu, X.H. Tang, Crack coalescence between two non-parallel flaws in rock-like material under uniaxial compression, Eng. Geol. 199(2015), pp74-90.

[6] Sheng-qi Yang, Hong-wen Jing, Tao Xu. Mechanical behavior and failure analysis of brittle sandstone specimens containing combined flaws under uniaxial compression. Journal of Central South University. 2014, Volume 21, pp2059–2073.

[7] Qian Yin, Hongwen Jing, and Haijian Su.Investigation on mechanical behavior and crack coalescence of sandstone specimens containing fissure-hole combined flaws under uniaxial compression. Geosciences JournalGJ. The Association of Korean Geoscience Societies and Springer 2018.

[8] Lu Zu-de, Ding Wu-xiu, Feng Xia-ting, ZHANG You-liang. Experimental study on mechanical-hydraulic-chemical coupling processing cracked rocks [J]. Chinese Journal of rock mechanics and Engineering, 2008, 27(4): 796-804. (in Chinese)

[9] Feng, X.T., Ding, W.X., and Zhang, D.X., 2009, Multi-crack interaction in limestone subject to stress and flow of chemical solutions. International Journal of Rock Mechanics and Mining Sciences, 46, pp159- 171.

[11] Cao R.H, P. Cao, H. Lin, C.Z.Pu, K.Ou. Mechanical behavior of brittle rock-like specimens with pre-existing fissures under uniaxial loading. Experimental studies and particle mechanics approach, Rock Mech. Rock Eng.49(3)(2016), pp763-783.

[11] Chen X., Z.H.Liao, X.Peeng, Deformability Characteristics of jointed rock masses under uniaxial compression, Int.J.Min. Sci. Technol. 22(2012), pp213-221

[12] Yang X.X., H.W.Jing,C.A. Tang, S.Q.Yang. Effect of parallel joint interaction on mechanical behavior of jointed rock mass models, Int.J.Rock Mech. Min. Sci.92(2017) pp40-53.

[13] Prudencio M., M. Van Sint Jan, Strength and failure modes of rock mass models with non-persistent joints, Int. J.Rock Mech. Min. Sci.44(20070890-902.

[14] Bahaaddini M., G.Sharrock, B.K. Hebblewhite. Numerical investigation of the effect of joint geometrical parameters on the mechanical properties of a non-persistent joi nted rock mass under uniaxial compression, Comput. Geotech. 49(2013) 2016-225.

[15] Fan X., P.H.S.W. Kulatilake, X.Chen. Mechanical behavior of rock-like jointed blocks with multi-non-persistent joints under uniaxial loading: a particle mechanics approach, Eng. Geol. 190(14)(2015), pp17-32.

[16] Itasca Consulting Group Inc., PFC3D Manual, Version 4.0. Minneapolis, Minnesota,2008.

[17] Yang XX, Kulatilake PHSW, Jing HW, Yang SQ. Numerical simulation of a jointed rock block mechanical behavior adjacent to an underground excavation and comparison with physical model test results. Tunn under space techn.2015;50, pp129-142.

[18] Li Y P, Chen L Z, Wang Y H. Experim ental research on pre-cracked marble under c ompression [J]. International Journal of Solids and Structures, 2005, 42, pp2505−2516.

[19] LABUZ J F, CATTANEO S, CHEN L H. Ac oustic emission at failure in quasi-brittle mater ials [J]. Construction and Building Materials, 2 001, 15, pp225−233.

[20] Chang S H, Lee C I. Estimation of crack ing and damage mechanisms in rock under tri axial compression by moment tensor analysis of acoustic emission [J]. International Journ al of Rock Mechanics and Mining Sciences, 2004, 41, pp1069−1086.

[21] Pestman B J, Van munster J G. An acoustic e mission study of damage development and st ress-memory effects in sandstone [J]. Intern ational Journal of Rock Mechanics and Mining Sciences & Geomechanics Abstracts, 1996, 3 3(6), pp585−593.